Celestial Mechanics and Dynamical Astronomy manuscript No.
(will be inserted by the editor)

Efficient design of direct low-energy transfers in multi-moon systems

Elena Fantino · Roberto Castelli

Received: date / Accepted: date

Abstract In this contribution, an efficient technique to design direct low-energy trajectories in multi-moon systems is presented. The method relies on analytical two-body approximations of trajectories originating from the stable and unstable invariant manifolds of two coupled circular restricted three-body problems. We provide a means to perform very fast and accurate computations of the minimum-cost trajectories between two moons. Eventually, we validate the methodology by comparison with numerical integrations in the three-body problem. Motivated by the growing interest in the robotic exploration of the Jovian system, which has given rise to numerous studies and mission proposals, we apply the method to the design of minimum-cost low-energy direct trajectories between Galilean moons, and the case study is that of Ganymede and Europa. However, the domain of applicability of the method is much wider. It can be employed, for instance, in geocentric orbit context, whenever a rendezvous or an orbit change is sought, in the optimization of high-energy patched-conics tours of multi-moon systems, and in the design of interplanetary deep space maneuvers.

1 Introduction

The objective of this paper is to present a method to determine the minimum-cost direct trajectories between libration points orbits of moons of a planetary system in the framework of the circular restricted three-body problem (CR3BP). The method is entirely analytical and offers conspicuous savings in computing time over traditional approaches based on intersecting invariant manifold trajectories. The motivation of the work is the contemporary interest in the *in situ* exploration of the planetary systems of the giant planets, and the consequent need for efficient trajectories enabling the execution of transfers or even tours

Elena Fantino
Space Studies Institute of Catalonia & Polytechnic University of Catalonia, Physics Department, Aeronautical Engineering Division, ESEIAAT, Colom 11, 08222 Terrassa, Spain.
E-mail: elena.fantino@upc.edu

Roberto Castelli
VU University Amsterdam, Department of Mathematics, De Boelelaan 1081, 1081 HV Amsterdam, The Netherlands.
E-mail: r.castelli@vu.nl

among their several moons. For example, ESA's JUICE mission (ESA, 2014), due to launch in 2022, will execute flybys at Callisto and Europa, and eventually shall orbit Ganymede. Then, NASA's Europa Mission plan (Lam et al., 2015) calls for a spacecraft to be launched to Jupiter in the 2020s: the probe would orbit the gas giant planet about every two weeks and execute close flybys of Europa. Prior to this, the cancelled JIMO project (Sims, 2006) was characterized by a reference trajectory with orbits around Callisto, Ganymede, and Europa. The widespread interest in the design of trajectories to explore the Jovian system was emphasized in the sixth edition of the Global Trajectory Optimisation Competition (GTOC6, Petropoulos, 2012), which focused on solving low-thrust multiple gravity-assist trajectories to map the Galilean moons. Notable contributions were given to the issue, e.g., Colasurdo et al. (2014); Izzo et al. (2013). These developments are all based on the multi-gravity assist technique applied to the two-body problem (patched conics) which allows long series of flybys at very low ΔV expense (on the order of tens of m/s).

By means of dynamical systems methods, it is possible to fly on low-energy trajectories departing from or leading to the vicinity of the libration points of the three-body problems composed by Jupiter and each of its moons. The first study of a low-energy tour of a planetary system is the Petit Grand Tour (PGT), applied to the exploration of the icy moons of Jupiter (Koon et al., 2000, 2002). The PGT exploits modern dynamical systems methods to compute global families of solutions with an almost arbitrary itinerary to explore the satellite system of any planet, to capture into orbit (temporary capture), depart, land or impact the various moons. The left side of Fig. 1 illustrates an example of a transfer from Ganymede to Europa with orbital capture. The model is the coupled CR3BP, built on the Jupiter-Ganymede CR3BP and the Jupiter-Europa CR3BP. The trajectories belonging to the two systems are connected through appropriately chosen Poincaré sections in the intermediate regions between the orbits of the two moons. The intersections are sought between unstable and stable manifolds of libration point orbits (LPOs, Gómez et al., 2003) of collinear libration points of the two systems. A PGT between Ganymede and Europa takes 25 days and less than half the amount of propellant employed in a Hohmann maneuver (which is characterized by a cost of 2.8 km/s). Further advances in low-energy trajectory design have led to the Multi-Moon Orbiter (MMO) concept (Ross et al., 2003; Koon et al., 2011), in which the spacecraft shifts from an orbit around one Jovian moon to an orbit around another. The ΔV requirements for such a mission can be very low (a few tens of m/s), provided the technique of low-energy inter-moon transfer is enhanced by resonant gravity assists. However, the time of flight accumulated in the inter-moon transfers is extremely long (several years). An example of such type of trajectories is shown in the right side of Fig. 1.

The aim of this paper is to illustrate an efficient method that can be applied, for instance, to design low-energy transfers between moons. The present work is motivated by the PGT concept, and has roots in a series of papers which laid the foundations of the low-energy transfers in the Sun-Earth-Moon system. In Koon et al. (2001), the transfer from a Low-Earth-Orbit to the Moon's vicinity is obtained by coupling the Sun-Earth and Earth-Moon CR3BPs and propagating the hyperbolic invariant manifolds of LPOs in the two systems in search for a low-ΔV intersections (see Fig. 2). Amongst others, key contributions in this line were given by Gómez et al. (2004); Zanzottera et al. (2012); Parker and Anderson (2014). In this paper, a system composed by a planet and two of its moons is considered and the coupled CR3BP is employed. Similarly to the PGT approach, we propagate the invariant manifolds of the planet-moon LPOs in the associated three-body model. However, far from the moons we approximate the invariant manifolds with Jupiter-centered Keplerian orbits and, by purely analytical arguments, we determine their intersections and the required manoeuvres. This approach offers two first advantages: it avoids the propagation of invariant

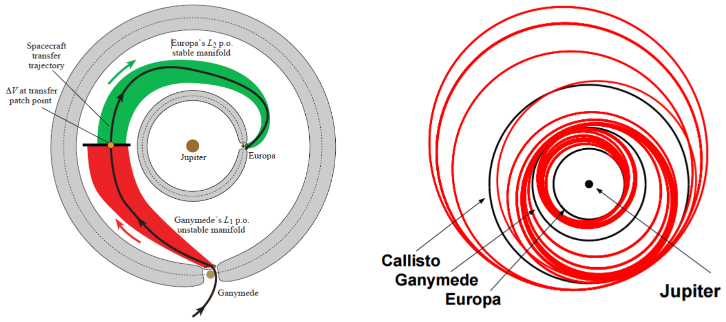

Fig. 1 Left: a Petit Grand Tour of the icy moons of Jupiter illustrating a transfer from Ganymede to Europa (Koon et al., 2002). Right: The Multi-Moon Orbiter concept for the Jovian moons involving resonant gravity assists with Callisto, Ganymede and Europa (Ross et al., 2003).

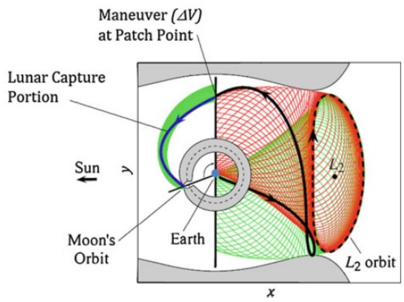

Fig. 2 The first low-energy transfer to the Moon obtained by coupling two CR3BPs: from a LEO to the vicinity of the L_2 point of the Sun-Earth CR3BP through the stable manifold of an LPO, then from there to a Poincaré section on a trajectory of the unstable manifold of the same LPO, and application of an impulsive maneuver (ΔV at patch point) to join a trajectory of the stable manifold of an LPO around the L_2 point of the Earth-Moon CR3BP (Koon et al., 2001).

manifolds in the inter-moon space, and it does not need to employ Poincaré sections to look for intersections between invariant manifolds.

In the resulting transfers, the inter-moon phase has a duration of a few days at most, and one large maneuver with magnitude at the level of 1 km/s is required. Therefore the result does not directly compare with the MMO nor with the more traditional high-energy trajectories based on multiple, intermediate encounters and small impulsive maneuvers. It does compare, instead, with the PGT and with the Hohmann maneuver.

The paper is organized in the following way: Section 2 defines the dynamical model, Section 3 describes the method, while Section 4 presents the application to transfers between Ganymede and Europa. The discussion and the conclusions follow in Section 5.

2 The model

The study is conceived in the context of the CR3BP (Szebehely, 2012) with the primaries being the planet (e.g., Jupiter) and one of its moons (e.g., one of the Galilean moons), while the third, massless body is the spacecraft. Figure 3 defines the synodical barycentric reference frame adopted in this work: the larger primary occupies the position (μ,0) and the

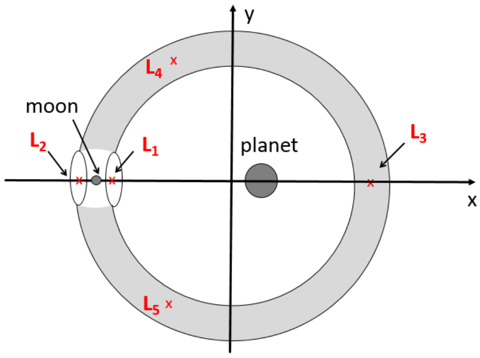

Fig. 3 The synodical baricentric reference frame of the CR3BP with the larger primary (the planet) to the right of the origin. The position of the five libration points is shown. The picture is completed by two Lyapunov orbits, respectively around L_1 and L_2, and the forbidden region (in grey) corresponding to their energy level.

smaller primary lies at $(\mu - 1, 0)$, μ being the mass ratio. In the following, the planar approximation is assumed because it is applicable in many real situations. For example, the relative inclinations between the orbital planes of the four Galilean moons are much smaller than one degree, hence their four orbits are approximately contained in one plane.

We aim at constructing trajectories connecting two moons revolving on consecutive orbits. Therefore, a connection between two CR3BPs is required. Such link is carried out in the so-called coupled CR3BP (Koon et al., 2011; Castelli, 2012), according to which the involved CR3BPs do not affect each other from the dynamical viewpoint, being their relationship merely a kinematical one. The coupling is constituted by the appropriate transformation of coordinates between the two synodical barycentric frames. In the quoted papers, the two restricted models are directly connected, meaning that phase states (position and velocity vectors) in one synodical frame are transformed into phase states in the other synodical frame when a given section is reached. In the present work, the two CR3BPs are not directly connected because the planet-spacecraft (restricted) two-body model is used in the inter-moon space. This choice is justified if the masses of the moons are many orders of magnitude smaller than that of the planet. For example, the Galilean moons are four to five orders of magnitude less massive than Jupiter.

The natural coordinate system to adopt when describing the dynamics in a central force field is the inertial frame. In order to perform the coupling in this frame, we apply a change of coordinates from each synodical frame to the planet-centered inertial frame. The transformation implies a change of origin from the center of mass of the planet-moon CR3BP to the center of the planet, together with a rotation around the z-axis by the angle between the x-axis of the synodical frame and the X-axis of the inertial frame, and a change of scale from normalized to physical units. We remark that the overall coupling depends on two angles, namely the angles swept by the x-axes of the synodical frames relative to the X-axis of the inertial frame. Due to rotation invariance, the two angles are redundant. Indeed, we can choose to orient the inertial reference frame so that the X-axis coincides with the x-axis of one of the synodical frames at time $t = 0$. This allows to eliminate the dependence on one of the two angles. As a whole, the transformation has one degree of freedom, represented by the relative phase of the two moons. However, since the angular velocities of the two moons are constant and known, the relative angular position of the two moons at any fixed time can be equivalently adopted as a parameter. The angle α_0 between the x-axes of the two

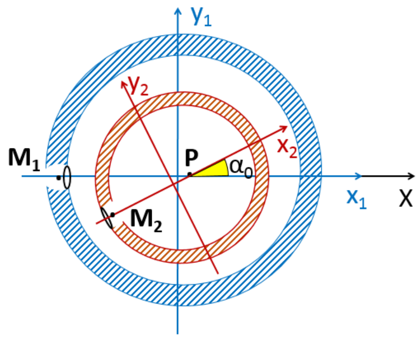

Fig. 4 The coupled CR3BP in a planetary system composed by planet P and two moons on consecutive orbits, M_1 the outer and M_2 the inner. The plot outlines the kinematical coupling at $t = 0$, which depends on the angle α_0 between the x-axes of the two synodical frames, as seen from an inertial observer. The x_1-axis is aligned with the X-axis of the inertial frame, as described in the text. For the sake of illustration, each synodical frame shows the forbidden region corresponding to the Jacobi constant value of the Lyapunov orbit around either L_1 or L_2.

synodical frames at time $t = 0$ is here employed to parameterise the coupled model. Figure 4 provides a schematic view of the relationship between the synodical frames at $t = 0$. The angle α_0 has a key role in the discussion that follows. Being a free parameter, upon discretisation it can be used to map the possible relative orientations between the two synodical frames in search for the optimal trajectory. Rather than systematically scanning and computing its values, we take advantage from the full integrability of the two-body problem and we analytically solve for the best α_0. Thus, only the optimal relative orientation will be considered for any choice of departure and arrival states.

We take the opportunity to observe that there exists a substantial difference between the coupled CR3BP of a planetary system, in which the linked problems both contain the dominant body, i.e., the planet, and the case of the Sun-Earth-Moon system in which the Earth-Moon CR3BP excludes the Sun and, therefore, the resulting coupled model does not always provide realistic solutions in the full four-body model (Fantino et al., 2010). Hence, the adoption of the coupled model within a planetary system not only is encouraged by the inherent simplicity, but also leads to results that can be easily refined to a high-fidelity model accounting for all the bodies involved.

3 The method

Given two moons on consecutive orbits, the transfer from the inner to the outer moon is intended as a trajectory leaving a planar Lyapunov orbit (PLO) around L_2 of the inner moon and ending at a PLO around L_1 of the outer moon. Viceversa, the transfer from the outer to the inner moon starts on a PLO around L_1 of the outer moon and ends at a PLO around L_2 of the inner moon. A PLO is escaped on a trajectory belonging to its unstable invariant manifold, whereas a PLO is approached via its stable invariant manifold. The PLOs are varied according to a certain energy discretization, leading to a database of orbits to be used in the trajectory design.

In the proposed method, the CR3BP is considered in the vicinity of the moon only, i.e., when the spacecraft-to-moon distance is small. For this purpose, we define a gravitational

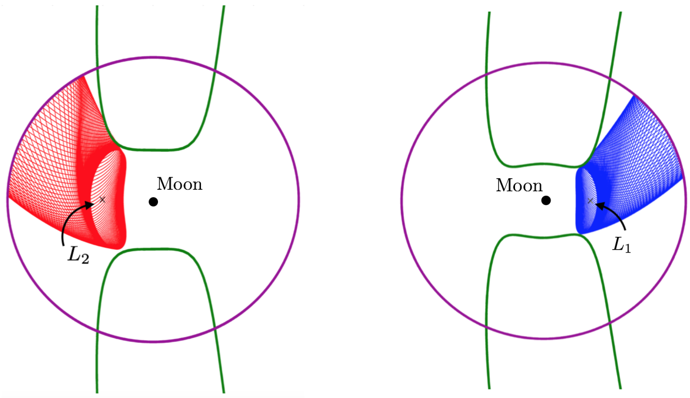

Fig. 5 Left: propagation of the unstable manifold of a PLO around the L_2 point of a moon-planet CR3BP till intersection with the circle of influence. Right: the same, but with a stable manifold of an LPO around the L_1 point. A portion of the border of the forbidden region associated to each PLO has also been drawn.

domain, limited by a so-called *circle of influence* (CI) centered at the moon and having a radius r_{CI} equal to the radius of the Laplace sphere (Roy, 1988) multiplied by a convenient factor k:

$$r_{CI} = k \times r_o \left(\frac{m}{M}\right)^{2/5}. \tag{1}$$

Here, r_o is the orbital radius of the given moon, m its mass and M the mass of the planet. The factor k is selected in such a way that the CI encircles, with due margin, all the Lyapunov orbits of the database. The CI is used, like a Poincaré section, to cut the flow of the stable or unstable manifolds associated to the selected PLOs (see Fig. 5).

The two-body approximation in a planet-centered inertial frame substitutes the CR3BP when dealing with the spacecraft's dynamics beyond the CI. Accordingly, the phase states collected on the CIs are transformed to the planet-centered inertial reference frame, and considered as initial conditions for backward/forward Keplerian orbit propagation. No matter the time direction, these Keplerian orbits are ellipses with a focus at the planet's center. Any Keplerian orbit is uniquely determined by the five classical orbital elements, i.e., semimajor axis a, eccentricity e, inclination i, right ascension of the ascending node Ω, and argument of pericenter ω, supplemented by the true anomaly θ that parameterises the motion along the ellipse. In planar approximation, the inclination and the right ascension of the ascending node are irrelevant, hence ω is measured from the X axis to the pericenter of the ellipse, and the so-called *Keplerian elements set* just consists of a, e, ω, and θ (Fig. 6).

Remark 1 We observe that the semimajor axis and the eccentricity provide the shape of the ellipse, and as such are fixed for a given state on the CI. On the contrary, the argument of pericenter depends on the orientation of the synodical frame of the given CR3BP in the XY-plane at the given time. More precisely, a change $\Delta\alpha$ in the orientation of the synodical frame produces an equivalent change $\Delta\omega$ of the argument of pericenter of the resulting ellipse. For the proof, the reader is referred to Appendix A.

Given two moons, the procedure for detecting possible connections is now sketched. For a choice of two LPOs, one on each CRTBP, upon discretization, some trajectories on the unstable and stable manifolds are integrated until the corresponding CI. Then, for a choice of α_0, the phase states collected on the two CIs are transformed into the corresponding

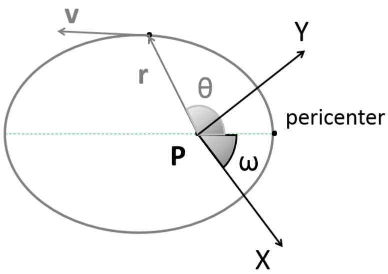

Fig. 6 An elliptical orbit with focus at the center of the planet (P). Its orientation in the orbital plane is defined by the argument of the pericenter ω, i.e., the angle between the X-axis of a planet-centered inertial frame and the pericenter of the ellipse. The position $\mathbf{r}$ and velocity $\mathbf{v}$ of a point of true anomaly θ are also shown.

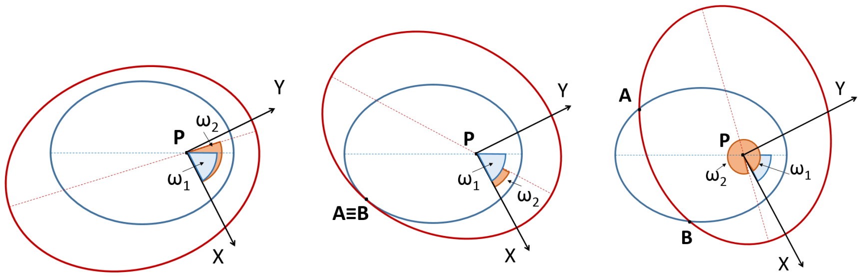

Fig. 7 Possible intersections between two ellipses with common focus (P): none, two identical (tangent ellipses $A \equiv B$) and two distinct ($A \neq B$), respectively on the left, center and right. ω_1 and ω_2 are the arguments of pericenter of the two ellipses and are measured from the X-axis of the inertial frame with origin at P.

Keplerian elements sets. Each set refers to an elliptical orbit travelled by the spacecraft under the gravitational influence of the planet. Connections between the two moons are then sought by looking at geometrical intersections between all possible combinations of ellipses emanating from the two CIs. In general, two ellipses possess at most four intersections. In our case, since the two ellipses have one common focus, i.e., the center of the planet, the number of intersections range from zero (i.e., no intersection) to two (i.e., two distinct points), with the case of one intersection corresponding to tangent ellipses (Fig. 7).

If an intersection between two ellipses exists, the magnitude ΔV of the difference in velocity at the intersection is the magnitude of the impulse to be applied by the propulsion system of the spacecraft to move from one orbit to the other, and eventually accomplish the transfer from a PLO of one planet-moon CR3BP to a PLO of the other planet-moon CR3BP. In the case of two distinct intersections, ΔV is not the same at the two points, although the difference is rather small. Figure 8 shows the two ways one can reach the CI of moon 2 (M_2) from the CI of moon 1 (M_1), i.e., through either A or B. The times of flight are, of course, very different.

The outlined procedure must be repeated for all the Lyapunov orbits of the database in each CR3BP and requires varying α_0 from 0 to 2π according to some discretization. Eventually, a large number of Keplerian elements sets is obtained.

The comparison of the costs of all the combinations of ellipses allows to identify the cheapest trajectory, i.e., the minimum-cost direct transfer between the sets of Lyapunov or-

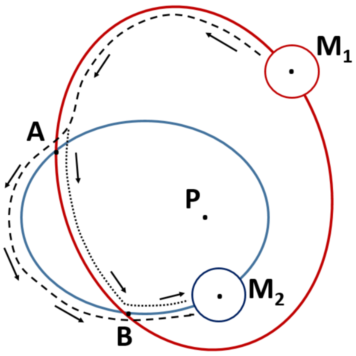

Fig. 8 The spacecraft leaves the CI of moon M_1 on an arc of ellipse that holds two distinct intersections with an arc of ellipse leading to the CI of moon M_2. The maneuver can be carried out at either A or B, which takes to two different paths, as indicated by the dashed and the dotted lines, respectively.

bits of the two given planet-moon systems. Performing the comparison requires computing the ΔV's of the several orbit pairs. This may become a time-consuming task if the resolution taken to discretize the angle α_0, the individual Lyapunov orbits and the Jacobi constant is narrow: at every new value of α_0, the intersections of the resulting Keplerian orbits must be determined and quantified. However, a closer look allows to simplify the problem and reduce the amount of computations. In the first place, the determination of ΔV is straightforward if the ellipses are described in polar coordinates in the respective planet-centered perifocal reference frames. The starting point is the polar equation of the ellipse, providing the distance r to the focus as a function of the true anomaly θ:

$$r = \frac{a(1-e^2)}{1+e\cos\theta}. \tag{2}$$

The intersections between two ellipses represented by the Keplerian elements sets (a_1, e_1, ω_1) and (a_2, e_2, ω_2), respectively, are obtained by solving

$$\frac{a_1(1-e_1^2)}{1+e_1\cos\theta_1} = \frac{a_2(1-e_2^2)}{1+e_2\cos\theta_2} \tag{3}$$

in which θ_1 and θ_2 are the true anomalies of the intersection points on the two curves. As shown in Fig. 9, θ_1 and θ_2 are related by

$$\theta_2 = \theta_1 - (\omega_2 - \omega_1) = \theta_1 - \Delta\omega. \tag{4}$$

$\Delta\omega$ thus represents the relative orientation between the two ellipses, i.e., the angle between the respective pericenters. System (3)-(4) admits solutions if and only if the discriminant of the associated second-degree algebraic equation (in $\cos\theta_1$, for example) is positive (see Appendix B for the full derivation). Once the true anomalies θ_1 and θ_2 of a point of intersection on the two ellipses have been found, the corresponding ΔV is determined as

$$\Delta V = \sqrt{(\dot{r}_1 - \dot{r}_2)^2 + (r\dot{\theta}_1 - r\dot{\theta}_2)^2}, \tag{5}$$

where r is the radial distance to the point of intersection, $\dot{r}_i$ (i = 1,2) are the radial velocities,

$$\dot{r}_i = \frac{a_i(1-e_i^2)e_i\sin\theta_i\dot{\theta}_i}{(1+e_i\cos\theta_i)^2} = \frac{r^2 e_i\sin\theta_i\dot{\theta}_i}{a_i(1-e_i^2)}, \tag{6}$$

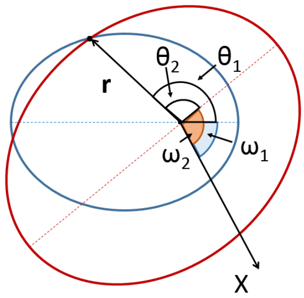

Fig. 9 The relationship between the difference in true anomaly of the same point belonging to two intersecting ellipses and the difference between the arguments of pericenter of the two curves.

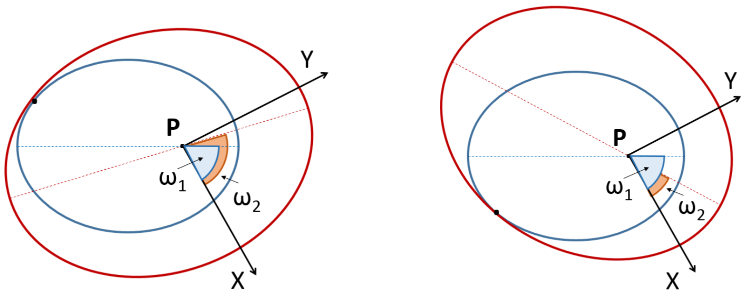

Fig. 10 The two orientations at which two ellipses are mutually tangent.

and $\dot{\theta}_i$ (i = 1,2) the angular velocities,

$$\dot{\theta}_i = \frac{h_i}{r^2}. \tag{7}$$

$h_i = \sqrt{GMa_i(1-e_i^2)}$ (i = 1,2) are the magnitudes of the specific orbital angular momenta and GM is the gravitational parameter of the planet.

Regarding the existence of the intersections, the requirement that the discriminant of the above mentioned second-degree equation is positive translates into an inequality to be satisfied by $\Delta\omega$, i.e., the two ellipses intersect only at certain relative orientations, represented by an interval of values for $\Delta\omega$:

$$\tau \leq \Delta\omega \leq 2\pi - \tau, \tag{8}$$

with $\tau \in [0, 2\pi[$. The value of τ depends only on the shape of the two ellipses and can be explicitly calculated in terms of a_i and e_i (i = 1,2). If $\tau > 0$, the domain of intersection is limited by the two orientations at which the ellipses are mutually tangent (Fig. 10). Such orientations are given by $\Delta\omega = \tau$ and $\Delta\omega = 2\pi - \tau$. On the other hand, if τ is zero, the two ellipses have two intersections regardless their relative orientation, and they can never be mutually tangent.

Our intuition suggests that for a choice of the shape of two ellipses, the cheapest connection is achieved when the ellipses are tangent. In order to prove it, we performed a parametric study of the behavior of ΔV as a function of $\Delta\omega$ for a large number of pairs of ellipses, with

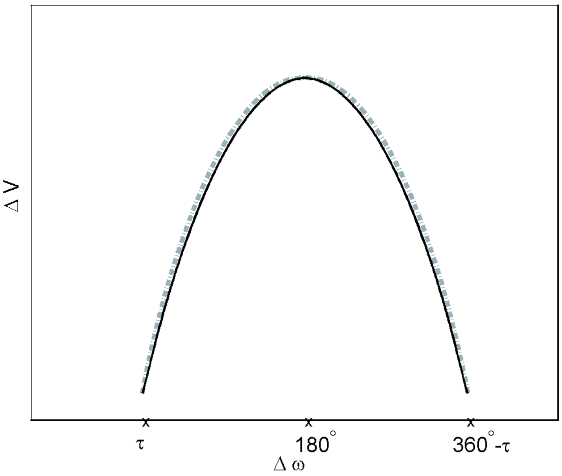

Fig. 11 ΔV at the intersections between two ellipses versus their relative orientation, represented by the angle $\Delta\omega$. The two curves (continuous and dashed, respectively) represent the ΔV at the two distinct intersection points and as such are limited by the two values of $\Delta\omega$ for which the ellipses are mutually tangent, respectively τ and $2\pi - \tau$. In these points the cost is the same at the two intersections since they coincide.

varying semimajor axis and eccentricity. For each pair, we determined τ, we made $\Delta\omega$ vary between τ and $2\pi - \tau$ and we computed ΔV at every intersection. The results show that if $\tau > 0$, ΔV has two equal minima when $\Delta\omega$ lies at either limit of the domain, i.e. when the two ellipses are mutually tangent. For all other values of $\Delta\omega$, the cost is higher. In particular, ΔV is maximum when the two apse lines are opposite ($\Delta\omega = \pi$), see Fig. 11. This behavior occurs at least when the orbital eccentricities are smaller than 0.2. Now, since the ellipses under study are an extension of the motion originating in the vicinity of the libration points, their path in inertial space must be geometrically quite similar to that of the associated equilibria (which move in circles). Hence, these orbits are expected to have low eccentricities, which guarantees the applicability of the intersection pattern of Fig. 11. Also note that a simple geometrical consideration allows to *a priori* discard the pairs of ellipses in which the pericenter distance of the outer ellipse is larger than the apocenter distance of the inner ellipse.

In conclusion, when looking for optimal low-cost transfers, only the orientation $\Delta\omega = \tau$ and $\Delta\omega = 2\pi - \tau$ at which the ellipses of a pair are mutually tangent must to be retained and evaluated because any other orientation corresponds to higher values of ΔV. From the relative orientation of the two ellipses, their Keplerian elements and the integration time of the selected trajectories on the stable and unstable manifolds, one *a posteriori* determines the initial relative phase α_0 of the two moons at time $t = 0$. This technique brings important savings in computing time above a brute force approach in which all the orientations are tried. Furthermore, the determination of τ is completely analytical.

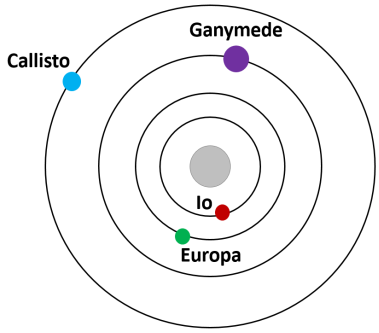

Fig. 12 The orbits of the four Galilean moons.

Table 1 The second and third column provide the orbital radii (in km) and the orbital periods (in days) of the four Galilean moons (first column). The fourth column lists the mass ratios $m_i/(m_i + m_J)$, with m_i the mass of the moon and $m_J = 0.189813 \cdot 10^{28}$ kg the mass of Jupiter.

Moon	Orbital radius (10^5 km)	Orbital period (days)	Mass ratio (10^{-4})
Io	4.2180	1.8	0.470542991630
Europa	6.7110	3.6	0.252865845179
Ganymede	10.7040	7.2	0.780632933465
Callisto	18.8270	16.7	0.566808592975

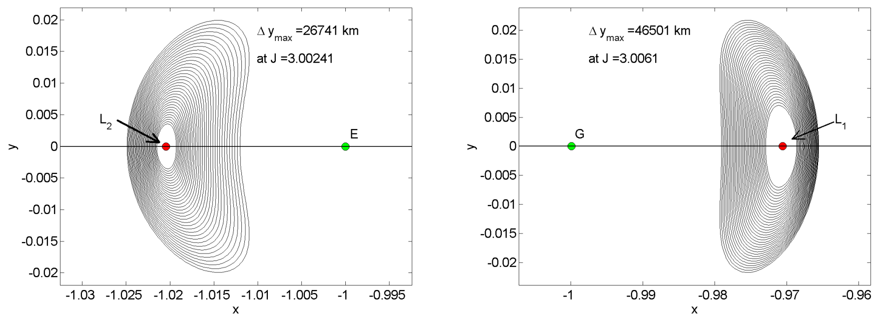

Fig. 13 The database of PLOs around L_2 in the Jupiter-Europa CR3BP (left) and around L_1 in the Jupiter-Ganymede CR3BP (right). The orbits are shown in the respective synodical barycentric reference frame. The value J of the Jacobi constant and the y-amplitude of the largest orbit in each set are reported.

4 Application: from Europa to Ganymede and viceversa

We present an application to the case of transfers between two Galilean moons, Europa and Ganymede. The orbits of the four main satellites of Jupiter are drawn to scale in Fig. 12 and their relevant orbital parameters are reported in Table 1.

The transfers connect two PLOs, one around the L_1 point of Jupiter-Ganymede and one around the L_2 point of Jupiter-Europa. Then, when designing a connection from Europa to Ganymede, the unstable invariant manifold of the Jupiter-Europa PLO is propagated to the CI around Europa, and the stable invariant manifold of the Jupiter-Ganymede PLO is propagated to the CI around Ganymede. The stability is reversed when dealing with transfers from

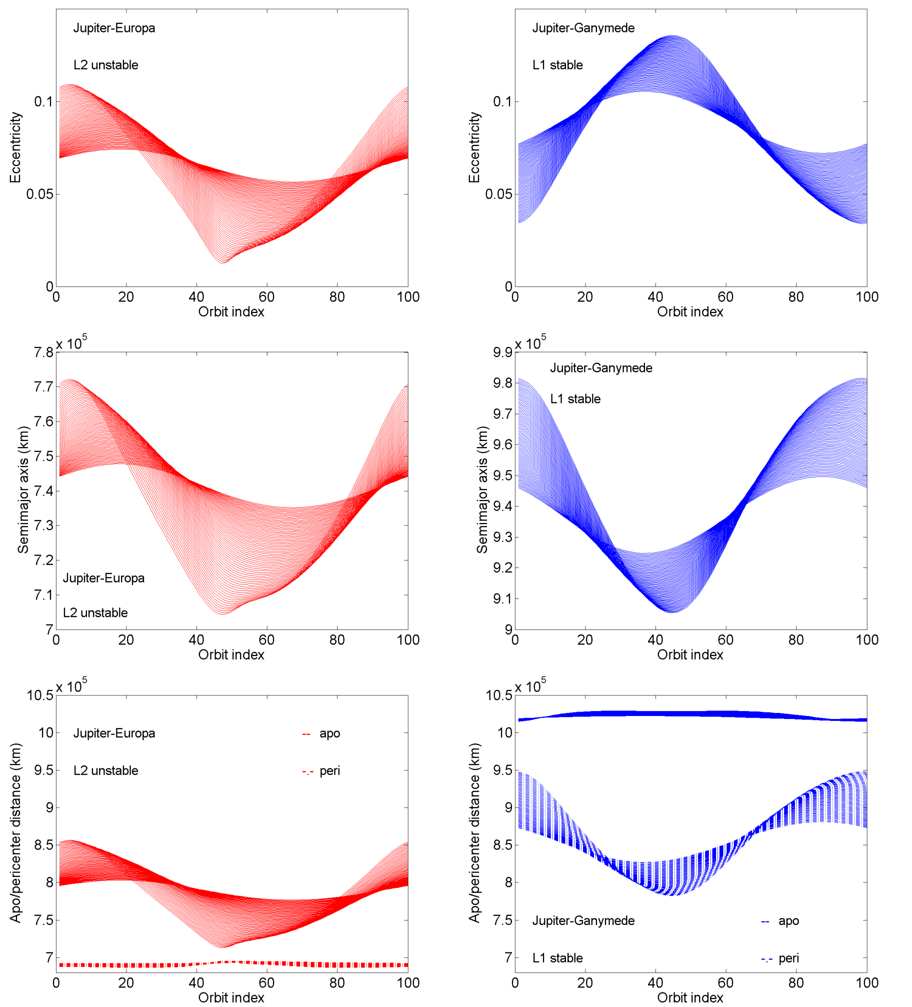

Fig. 14 Eccentricites (top), semimajor axes (middle) and apojove/perijove distances (bottom) of the ellipses with focus at Jupiter leaving the CIs of Europa (left) and Ganymede (right) and coming from PLOs around L_2 or leading to PLOs around L_1, respectively. The several curves in each subplot give the values of the specified parameter on the different LPOs of the database as functions of the discretization index on each LPO.

Ganymede to Europa. The CIs around Europa and Ganymede have radii of 38905 km and 97409 km, respectively, both corresponding to $k = 4$. The PLOs are taken from a database of 70 orbits in each system (see Fig. 13). For the sake of illustration, a discretization of the PLOs with 100 points is adopted. Already at this moderate resolution, 100 points per orbit mean 7000 manifold trajectories in each CR3BP, since all the PLOs of the database must be tried. The intersections of each trajectory with the corresponding CI provides a set of Keplerian elements in the Jupiter-centered inertial frame. In principle, from the resulting ellipses, 49 million possible pairs are formed. However, only the pairs in which the perijove distance of the outer ellipse is smaller than the apojove distance of the inner ellipse must be retained. The others have zero intersections. For both Europa-to-Ganymede and Ganymede-to-Europa

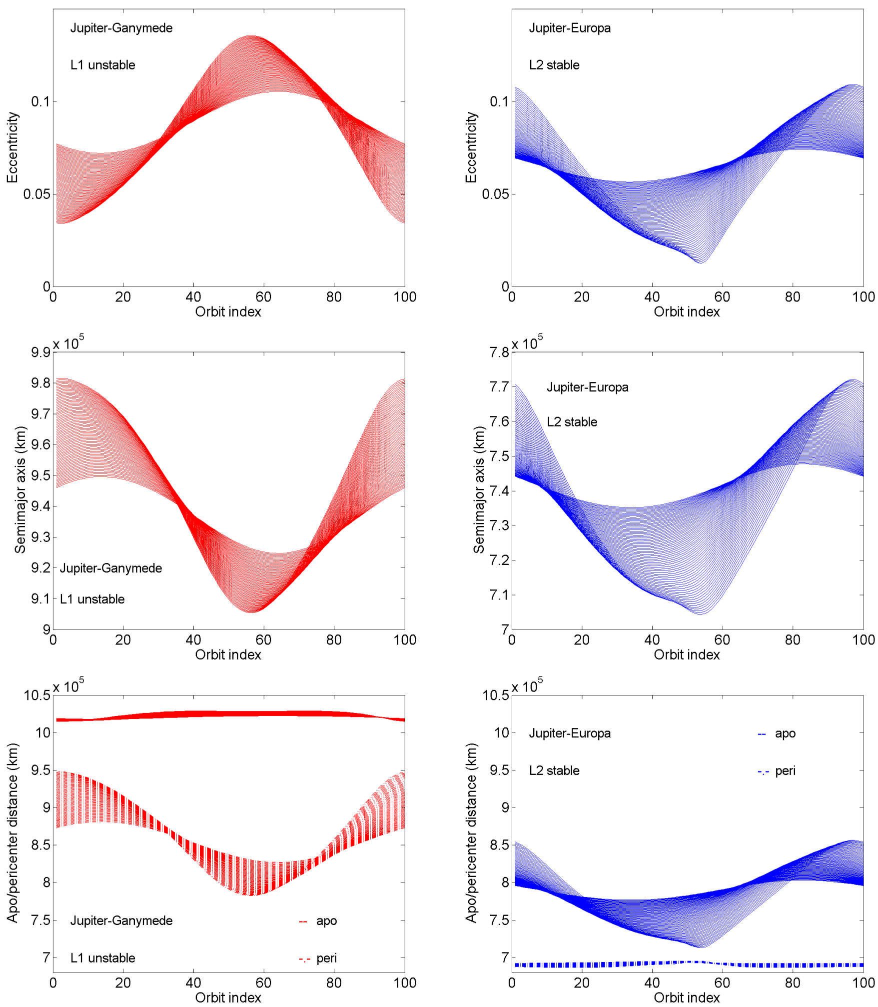

Fig. 15 Eccentricites (top), semimajor axes (middle) and apojove/perijove distances (bottom) of the ellipses with focus at Jupiter leaving the CIs of Ganymede (left) and Europa (right) and coming from PLOs around L_1 or leading to PLOs around L_2, respectively. The several curves in each subplot give the values of the specified parameter on the different LPOs of the database as functions of the discretization index on each LPO.

connections, the number of pairs to be analysed is of approximately 3.8 million, corresponding to 8% of the initial amount. Figure 14 maps the eccentricites, the semimajor axes and the apojove and perijove distances of the ellipses originating, respectively, from the unstable manifolds of the Jupiter-Europa PLOs and the stable manifolds of the Jupiter-Ganymede PLOs. Similarly, Fig. 15 shows the eccentricites, the semimajor axes and the apojove and perijove distances of the ellipses originating, respectively, from the stable manifolds of the Jupiter-Europa PLOs and the unstable manifolds of the Jupiter-Ganymede PLOs. The orbital eccentricities are always smaller than 0.14, thus enabling the application of the algorithm described in Sect. 3. Besides, all the pairs of ellipses have a strictly positive value of τ, meaning that the orientation for which the ellipses of a pair are mutually tangent always

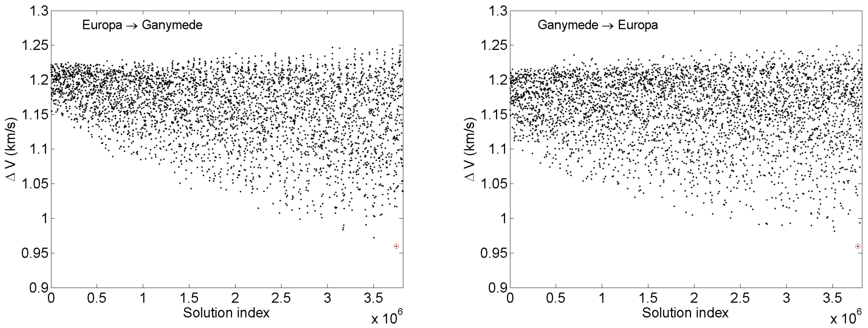

Fig. 16 The cost of the cheapest LET transfers from Europa to Ganymede (left) and from Ganymede to Europa (right) as functions of the combination index (running from 1 to 3.8 million). The absolute minima have been marked with a red circle (bottom right).

exists, and constitutes the minimum-cost orientation for each pair. ΔV ranges from 0.960 km/s to 1.257 km/s for both transfers (Fig. 16), i.e. from Europa to Ganymede and from Ganymede to Europa. In particular, 0.960 km/s is the absolute minimum in both directions. The Europa-to-Ganymede and Ganymede-to-Europa minimum-cost trajectories are shown in Fig. 17. The spacecraft is at the numbered positions of the Europa-to-Ganymede transfer (left subplot) at times t_0 = 0, t_1 = 3.33 days, t_2 = 5.84 days, t_3 = 8.27 days, t_4 = 14.48 days, respectively. As for the Ganymede-to-Europa transfer (right subplot), the spacecraft is at the numbered positions at times t_0 = 0, t_1 = 6.21 days, t_2 = 8.64 days, t_3 = 11.15 days, t_4 = 14.48 days, respectively. Thus, the two transfers are characterized by the same time of flight.

With the adopted discretization, there is no cheaper direct transfer connecting PLOs in the two systems. The Lyapunov orbits involved in these two minimum-cost trajectories are the largest in either database, i.e., they are the PLOs with the lowest Jacobi constant in the set (3.0061 and 3.0024, respectively for Ganymede and Europa). The fact that the two optimal transfers require the same ΔV and employ the same time of flight is not accidental, and can be explained by combining geometrical arguments for the Keplerian ellipses and the time-space symmetry of the CR3BP.

For the sake of completeness, in Fig. 18 we show the minimum-cost trajectories obtained by applying the method to the low-energy transfers (LETs) between Io and Europa (ΔV = 1.294 km/s, time of flight = 7.52 days) and between Ganymede and Callisto (ΔV = 1.003 km/s, time of flight = 31.88 days), both outwards and inwards. The meaning of line styles, symbols and labels is the same as in Fig. 17.

5 Discussion and conclusions

We have verified the physical validity of the solutions by propagating the initial state on the PLO around L_2 of Europa forward in time to the maneuver point in the Jupiter-Europa CR3BP, and the final state on the PLO around L_1 of Ganymede backwards in time to the maneuver point in the Jupiter-Ganymede CR3BP. The propagation time is of 5.84 days over the former segment and 8.64 days over the latter. The distance between the endpoints of the two segments is of 7000 km, which is equivalent to the accumulation of a speed error of 6 m/s over the whole transfer (7000 km / 14.48 days). This error, due to the Keplerian approx-

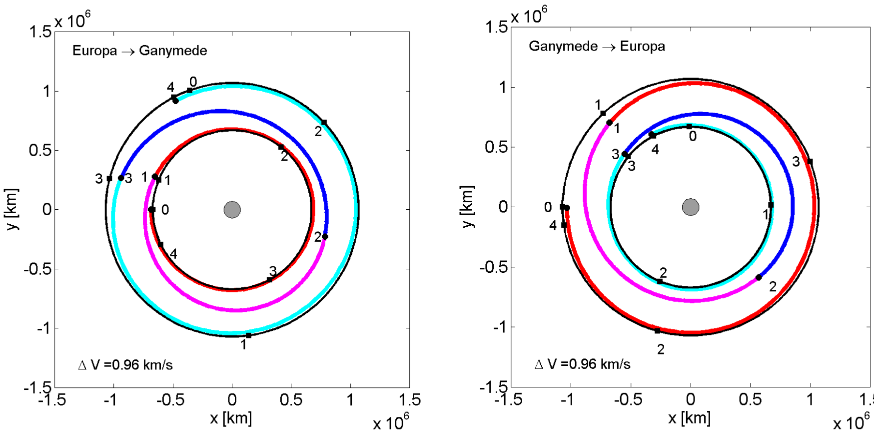

Fig. 17 Illustration of the Europa-to-Ganymede (left) and Ganymede-to-Europa (right) transfers with the lowest cost, i.e. 0.960 km/s. The trajectories are drawn in Jupiter-centered inertial coordinates. The thin black lines are the orbits of the two moons, the thick coloured lines are the several arcs followed by the spacecraft: in red the trajectory belonging to the unstable invariant manifold, in magenta and blue the portions of the two Keplerian ellipses, in cyan the trajectory belonging to the stable invariant manifold. Labels indicate the positions of the spacecraft (filled circles) at the beginning of each arc. The positions of the two moons (filled squares) at the same moments are also labelled. The filled circle denoted by number 2 is the maneuver point.

imation of the CR3BP model, is negligible when compared with the size of the computed maneuver (0.96 km/s).

The numerical code has been written in Fortran language and compiled with Intel Visual Fortran Composer XE 2013 SP1 under Microsoft Visual Studio Professional 2013. All computations have been performed on a Lenovo laptop computer with Intel Core i5-3230M processor with 2.6 GHz CPU and Windows 8.1 Enterprise operating system. Computations are performed in two phases. In the pre-processing phase, the PLOs are propagated and discretized, the stable and unstable invariant manifolds are propagated till intersection with the CIs, the end states are transformed into Keplerian elements sets which are then stored. This phase takes on the order of ten seconds, but is executed only once. In the second phase, the minimum-cost intersections of the 49 million pairs of ellipses of a transfer, e.g., from Europa to Ganymede, are determined and sorted with respect to cost, the cheapest trajectory is identified and traced. The time required for the second phase is lower than one second, most of which is spent in reading and writing data. It should be noted that the majority of the pairs are rejected on the basis of the perijove-apojove criterion and are not evaluated. This is a merit of the method, and an advantage made possible by the Keplerian approximation. Another important geometrical feature of the Keplerian approach is the fact that the configuration in which two ellipses are mutually tangent exists for all the pairs. This enables the application of the method to all the cases. Besides, the computations are entirely analytical and explicit, no numerical approximation is made (except for the invariant manifolds propagation executed in the pre-processing phase) and no intrinsic procedures are called.

The minimum-cost solutions, like those illustrated in Figs. 17 and 18, require the occurrence of specific values of α_0, i.e., specific relative orbital geometries between the moons at the time of departure. Such geometries, and consequently the departure opportunities, repeat after intervals equal to the synodical period of the two moons. In the case of transfers between Europa and Ganymede, the synodical period is of 7.2 days. Solutions with cost

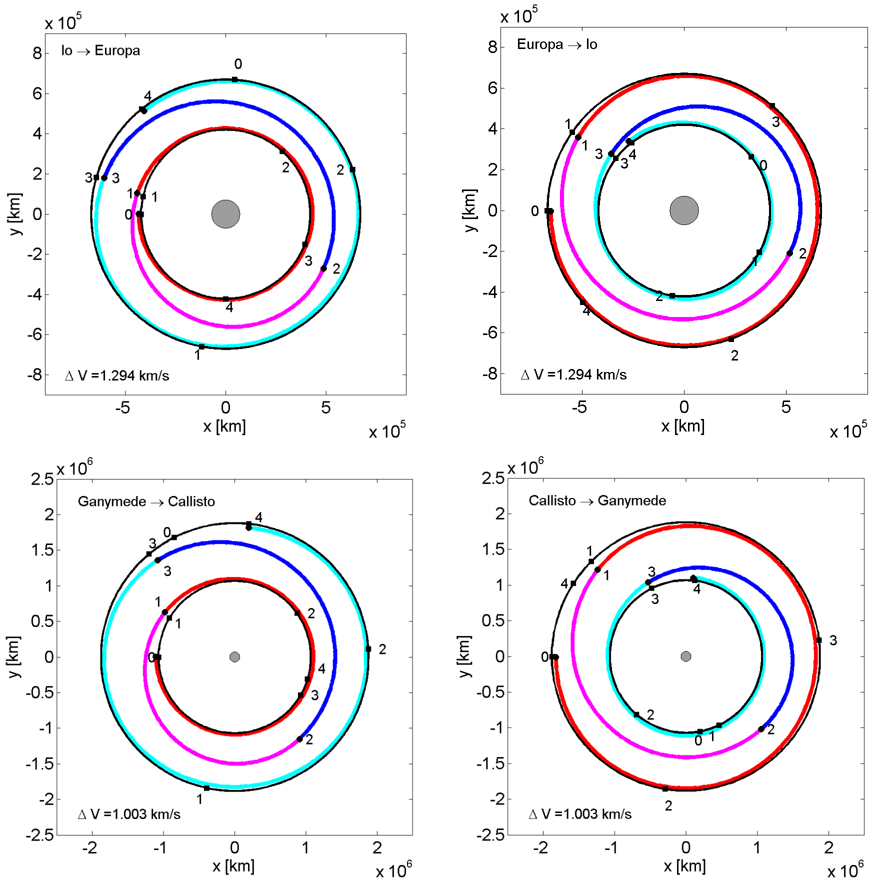

Fig. 18 Illustration of the minimum-cost transfer from Io to Europa (top left), from Europa to Io (top right), from Ganymede to Callisto (bottom left) and from Callisto to Ganymede (bottom right). The trajectories are drawn in Jupiter-centered inertial coordinates. The thin black lines are the orbits of the two moons, the thick coloured lines are the several arcs followed by the spacecraft: in red the trajectory belonging to the unstable invariant manifold, in magenta and blue the portions of the two Keplerian ellipses, in cyan the trajectory belonging to the stable invariant manifold. Labels indicate the positions of the spacecraft (filled circles) at the beginning of each arc. The positions of the two moons (filled squares) at the same moments are also labelled. The filled circles denoted by number 2 are the maneuver points. The cost is reported in the bottom left corner of each panel.

above the absolute minimum may be chosen if they correspond to more convenient values of α_0 relative to the mission requirements. So, in general the method lends itself to trade-offs between cost and other parameters (including the time of flight).

The costs found in the analysis of the solutions are at the level of 1 km/ and are large in comparison with those of the high-energy patched conics trajectories published in the literature. However, it should be noted that the proposed approach has been developed in a different dynamical model, i.e., that of low-energy transfers, and the resulting trajectories between moons are direct (hence fast). In this context, not only the method yields results in agreement with previous studies (Gomez et al., 2001), but it also identifies the minimum-cost solutions of this category. Besides, our large manouvers are perfectly attainable by means of electrical thrusters, which nowadays constitute a mature and widely used spacecraft technology.

The intense particle radiation environment that characterizes the Jovian magnetosphere, with dangerous fluxes reaching out almost to the orbit of Ganymede, may represent an obstacle to the practical implementation of trajectories that spend days in the inter-moon space. This same argument, unfortunately, applies even more to more traditional strategies. Therefore, we can conclude that Jupiter's radiation environment puts serious limitations to the feasibility of spacecraft tours of the Galilean moons. However, on the one hand, technology is developing fast and hardware hardening as well, which makes us confident that these trajectories will become viable in a few years from now. On the other hand, noticeable time-of-flight reductions can be obtained if transit orbits (which pass straight through the PLOs) are used instead of invariant manifold trajectories (which are known to spend a lot of time in the asymptotic motion to or from the PLOs). This modification to the method is currently under development and will be the subject of a future publication.

In conclusion, we have presented a method to determine the minimum-cost direct low-energy trajectories between libration point orbits of a multi-moon system. The method is entirely analytical and offers conspicuous savings in computing time over traditional approaches based on intersecting invariant manifold trajectories. We have illustrated the application of the method to the design of transfers between Galilean moons, with particular attention to the case of Europa and Ganymede. A final remark on the domain of applicability of the method here presented is due. The Keplerian approximation has been illustrated here in the context of the LETs between Jovian moons, but its capability is much wider: it can be employed in any context in which a dominant center of attraction is present: for instance, in the realm geocentric orbits, whenever a rendezvous or an orbit change is sought, in the optimization of high-energy patched-conics tours of multi-moon systems, and in the design of interplanetary deep space maneuvers.

Appendix A

In the following, we derive the relationship between two planet-centered ellipses generated by one and the same state vector on the CI at two different orbital phases of the moon. Let $\mathbf{s} = (x, y, \dot{x}, \dot{y})^T$ be a state vector on the CI in synodical coordinates. Denote by $\mathbf{S}_1 = (X_1, Y_1, \dot{X}_1, \dot{Y}_1)^T$ and $\mathbf{S}_2 = (X_2, Y_2, \dot{X}_2, \dot{Y}_2)^T$ two state vectors in the planet-centered inertial frame obtained by $\mathbf{s}$ when the orbital phases of the moon (i.e., the planet-centered angles from the X-axis to the location of the moon) are α_1 and α_2, respectively. Also, let Σ_1 and Σ_2 be the two elliptical orbits, with focus at the planet, passing through $\mathbf{S}_1$ and $\mathbf{S}_2$, respectively. In remark 1 it has been stated that Σ_1 and Σ_2 have the same shape (i.e., they have the same semimajor axis and eccentricity) and are related by a rotation of angle $\Delta\alpha = \alpha_2 - \alpha_1$, i.e., $\omega_2 = \omega_1 + \Delta\alpha$. We now provide a proof of the claim. Denoting $R(\alpha) = \begin{bmatrix} \cos\alpha & -\sin\alpha \\ \sin\alpha & \cos\alpha \end{bmatrix}$ the rotation matrix of angle α, we show that

i) $(X_2, Y_2)^T = R(\Delta\alpha)(X_1, Y_1)^T$
ii) $(\dot{X}_2, \dot{Y}_2)^T = R(\Delta\alpha)(\dot{X}_1, \dot{Y}_1)^T$.

i) Let us consider the trajectory passing through $\mathbf{s}$ at time $t = T$ in the rotating frame. In the same time units in the planet-centered inertial frame, the trajectory is given by

$$\begin{bmatrix} X \\ Y \end{bmatrix}(t) = \kappa R(\beta(t)) \begin{bmatrix} x \\ y \end{bmatrix}(t), \qquad (9)$$

where the constant κ is the scaling factor from normalized to physical units and $\beta(t) = \beta + t$, being β the relative phase of the rotating frame with respect to the inertial frame at time $t = 0$. If at time $t = T$ the orbital phase of the moon is α_i (i = 1,2), then the phase at time $t = 0$ is $\beta_i = \alpha_i - T$. Hence, in the planet-centered inertial frame we consider two trajectories

$$\begin{bmatrix} X_1 \\ Y_1 \end{bmatrix}(t) = \kappa R(\beta_1 + t) \begin{bmatrix} x \\ y \end{bmatrix}(t), \tag{10}$$

and

$$\begin{bmatrix} X_2 \\ Y_2 \end{bmatrix}(t) = \kappa R(\beta_2 + t) \begin{bmatrix} x \\ y \end{bmatrix}(t). \tag{11}$$

Since the rotations form a group, $R(\beta_2 + t) = R(\beta_1 + t + \Delta\alpha) = R(\Delta\alpha)R(\beta_1 + t)$. Thus,

$$\begin{bmatrix} X_2 \\ Y_2 \end{bmatrix}(t) = R(\Delta\alpha) \begin{bmatrix} X_1 \\ Y_1 \end{bmatrix}(t). \tag{12}$$

The last expression, evaluated at $t = T$, gives i). Differentiation and time units rescaling yield ii). This proof neglects the distance between the center of mass of the planet-moon system and the center of the planet. In the cases under study this distance does not exceed a few tens of km.

Appendix B

This appendix contains the algebraic computation of the intersection between two ellipses with one common focus. This represents the general, non-degenerate situation of the problem dealt with in this paper. Let us assume that the two Keplerian orbits are non-identical ellipses with $e_1, e_2 \neq 0$[1]. The point(s) of intersection between the two curves are obtained by developing the condition expressed in Eq. 3 with Eq. 4:

$$p_1 + p_1 e_2 \cos(\theta_1 - \Delta\omega) = p_2 + p_2 e_1 \cos\theta_1. \tag{13}$$

Here $p_i = a_i(1 - e_i^2)$ $(i = 1, 2)$ is the semilatus rectum of the ellipse. Substitution of $\cos(\theta_1 - \Delta\omega)$ with $\cos\theta_1 \cos\Delta\omega + \sin\theta_1 \sin\Delta\omega$ provides

$$a + b\cos\theta_1 = c\sin\theta_1, \tag{14}$$

where $a = p_1 - p_2$, $b = p_1 e_2 \cos\Delta\omega - p_2 e_1$ and $c = -p_1 e_2 \sin\Delta\omega$. Taking the square of Eq. 14 yields

$$(b^2 + c^2)\cos^2\theta_1 + 2ab\cos\theta_1 + a^2 - c^2 = 0, \tag{15}$$

or

$$k_1 \cos^2\theta_1 + 2k_2 \cos\theta_1 + k_3 = 0, \tag{16}$$

with $k_1 = b^2 + c^2$, $k_2 = ab$, $k_3 = a^2 - c^2$. Eq. 16 is a second-degree algebraic equation in $\cos\theta_1$. It has solutions if and only if the radicand $w = k_2^2 - k_1 k_3$ is positive or null. In this

[1] The case in which one or both ellipses are circles is trivial.

case, the true anomalies θ_{1A} and θ_{1B} of the two points A and B in the perifocal reference frame of ellipse 1 (see Fig. 7) are given by

$$\cos\theta_{1A} = \frac{-k_2 + \sqrt{w}}{k_1}, \tag{17}$$

$$\sin\theta_{1A} = \frac{a + b\cos\theta_{1A}}{c}, \tag{18}$$

$$\cos\theta_{1B} = \frac{-k_2 - \sqrt{w}}{k_1}, \tag{19}$$

$$\sin\theta_{1B} = \frac{a + b\cos\theta_{1B}}{c}. \tag{20}$$

Eqs. 18 and 20 become indefinite if $c = 0$ (the two apse lines either coincide, $\Delta\omega = 0$, or are oppositely oriented, $\Delta\omega = 180°$). In this case, Eq. 14 becomes

$$a + b\cos\theta_1 = 0, \tag{21}$$

which provides $\cos\theta_{1A} = \cos\theta_{1B} = -a/b$ with $\sin\theta_{1A} = \sqrt{1 - \cos^2\theta_{1A}}$ and $\sin\theta_{1B} = -\sin\theta_{1A}$.

Acknowledgements The authors wish to thank Martin Ozimek, Roberto Flores and Andrea Viale for useful discussions.

References

Castelli, R. (2012). Regions of prevalence in the coupled restricted three-body problems approximation. *Communications in Nonlinear Science and Numerical Simulation*, 17(2):804 – 816.

Colasurdo, G., Zavoli, A., Longo, A., Casalino, L. and Simeoni, F. (2014). Tour of Jupiter galilean moons: Winning solution of GTOC6. *Acta Astronautica*, 102:190–199.

ESA (2014). *JUICE JUpiter ICy moons Explorer*, volume 1. ESA.

Fantino, E., Gómez, G., Masdemont, J. J. and Ren, Y. (2010). A note on libration point orbits, temporary capture and low-energy transfers. *Acta Astronautica*, 67(9–10):1038–1052.

Gómez, G., Koon, W. S., Lo, M. W., Marsden, J. E., Masdemont, J. J. and Ross, S.D. (2001). Invariant manifolds, the spatial three-body problem and space mission design. *Advances in the Astronautical Sciences*, 109(AAS 01-301):3–22.

Gómez, G., Koon, W. S., Lo, M. W., Marsden, J. E., Masdemont, J. J. and Ross, S. D. (2004). Connecting orbits and invariant manifolds in the spatial restricted three-body problem. *Nonlinearity*, 17(5):1571.

Gómez, G., Masdemont, J. J. and Mondelo, J. (2003). Libration point orbits: a survey from the dynamical point of view. In Gómez, G., Lo, M. W., and Masdemont, J. J., editors, *Libration Point Orbits and Applications*. World Scientific Publishing Company.

Izzo, D., Simoes, L. F., Martens, M., de Croon, G. C. H. E., Heritier, A. and Yam, C. (2013). Search for a grand tour of the Jupiter galilean moons. In *Proceedings of the 15th annual conference on Genetic and evolutionary computation*, pages 1301–1308, Amsterdam, The Netherlands. ACM.

Koon, W. S., Lo, M. W., Marsden, J. E. and Ross, S. D. (2011). *Dynamical Systems, the Three-Body Problem and Space Mission Design*. Marsden Books.

Koon, W. S., Lo, M. W., Marsden, J. E. and Ross, S. D. (2000). Heteroclinic connections between periodic orbits and resonance transitions in celestial mechanics. *Chaos*, 10(2):427–469.

Koon, W. S., Lo, M. W., Marsden, J. E. and Ross, S. D. (2001). Low energy transfer to the moon. *Celestial Mechanics and Dynamical Astronomy*, 81:63–73.

Koon, W. S., Lo, M. W., Marsden, J. E. and Ross, S. D. (2002). Constructing a low energy transfer between jovian moons. *Celestial Mechanics, Dedicated to Donald Saari for his 60th Birthday*, page 129.

Lam, T., Camacho, J. A. and Buffington, B. (2015). The Europa mission: Multiple Europa flyby Trajectory Design Trades and Challenges. In *AAS/AIAA Astrodynamics Specialist Conference, Vail, Colorado*, number Paper No. AAS 15-657.

Parker, J. S. and Anderson, R. L. (2014). *Low-Energy Lunar Trajectory Design*. John Wiley & Sons, Inc.

Petropoulos, A. (2012). Problem description for the 6^{th} global trajectory optimisation competition. *http://www.esa.int/gsp/ACT/doc/ MAD/ACT-RPT-MAD-GTOC6-problem_stmt.pdf*.

Ross, S. D., Koon, W. S., Lo, M. W. and Marsden, J. E. (2003). Design of a multi-moon orbiter. In *13th AAS/AIAA Space Flight Mechanics Meeting. Ponce, Puerto Rico*, volume AAS 03-143.

Roy, A. E. (1988). *Orbital Motion, Third Edition*. Adam Hilger.

Sims, J. A. (2006). Jupiter icy moons orbiter mission design overview. In *AAS/AIAA Space-Flight Mechanics Meeting, Tampa, Florida*. Pasadena, CA : Jet Propulsion Laboratory, National Aeronautics and Space Administration.

Szebehely, V. (2012). *Theory of orbit: The restricted problem of three Bodies*. Elsevier Science.

Zanzottera, A., Mingotti, G., Castelli, R. and Dellnitz, M. (2012). Intersecting invariant manifolds in spatial restricted three-body problems: Design and optimization of Earth-to-halo transfers in the Sun–Earth–moon scenario. *Communications in Nonlinear Science and Numerical Simulation*, 17(2):832 – 843.